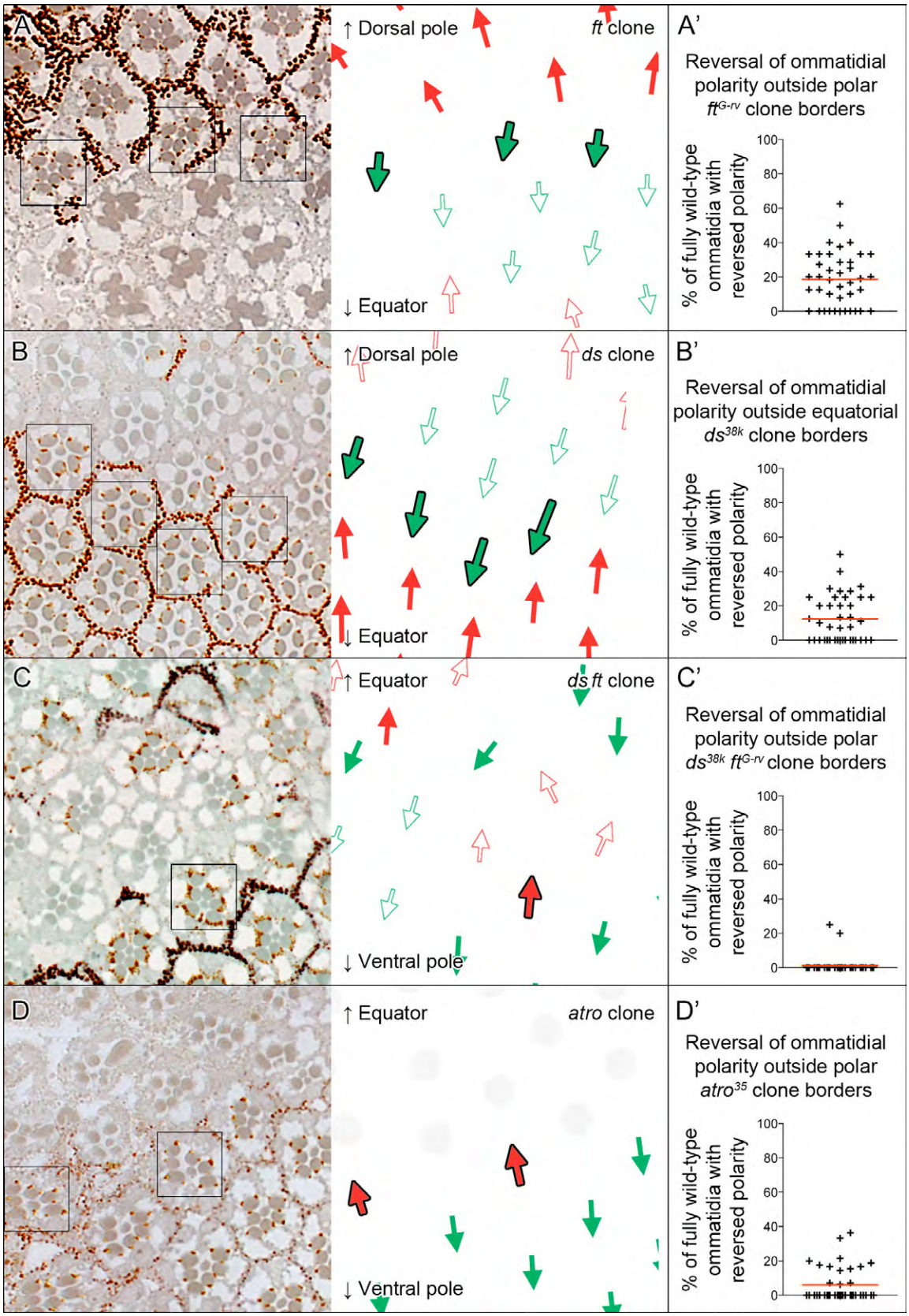

Fig. S1. Polarity reversals occur in fully wild-type ommatidia on clone borders. Polarity reversals in ommatidia with at least seven wild-type photoreceptors. In this figure, these fully wild-type ommatidia are enclosed in boxes in the sections, and are represented as solid arrows with a black outline to distinguish them from ommatidia that are $R3^+/R4^+$ but mosaic for other photoreceptors, which do not have the black outline. (A,A′) *ft* clones cause polarity reversals in 19% of fully wild-type ommatidia on the polar side (*n*=40 clones/331 ommatidia). (B,B′) *ds* clones cause polarity reversals in 12% of fully wild-type ommatidia on the equatorial side (*n*=40 clones/355 ommatidia). (C,C′) *ds ft* clones cause polarity reversals in 1% of fully wild-type ommatidia on the polar side (*n*=40 clones/288 ommatidia). (D,D′) *atro* clones cause polarity reversals in 6% of fully wild-type ommatidia on the polar side (*n*=38 clones/362 ommatidia).

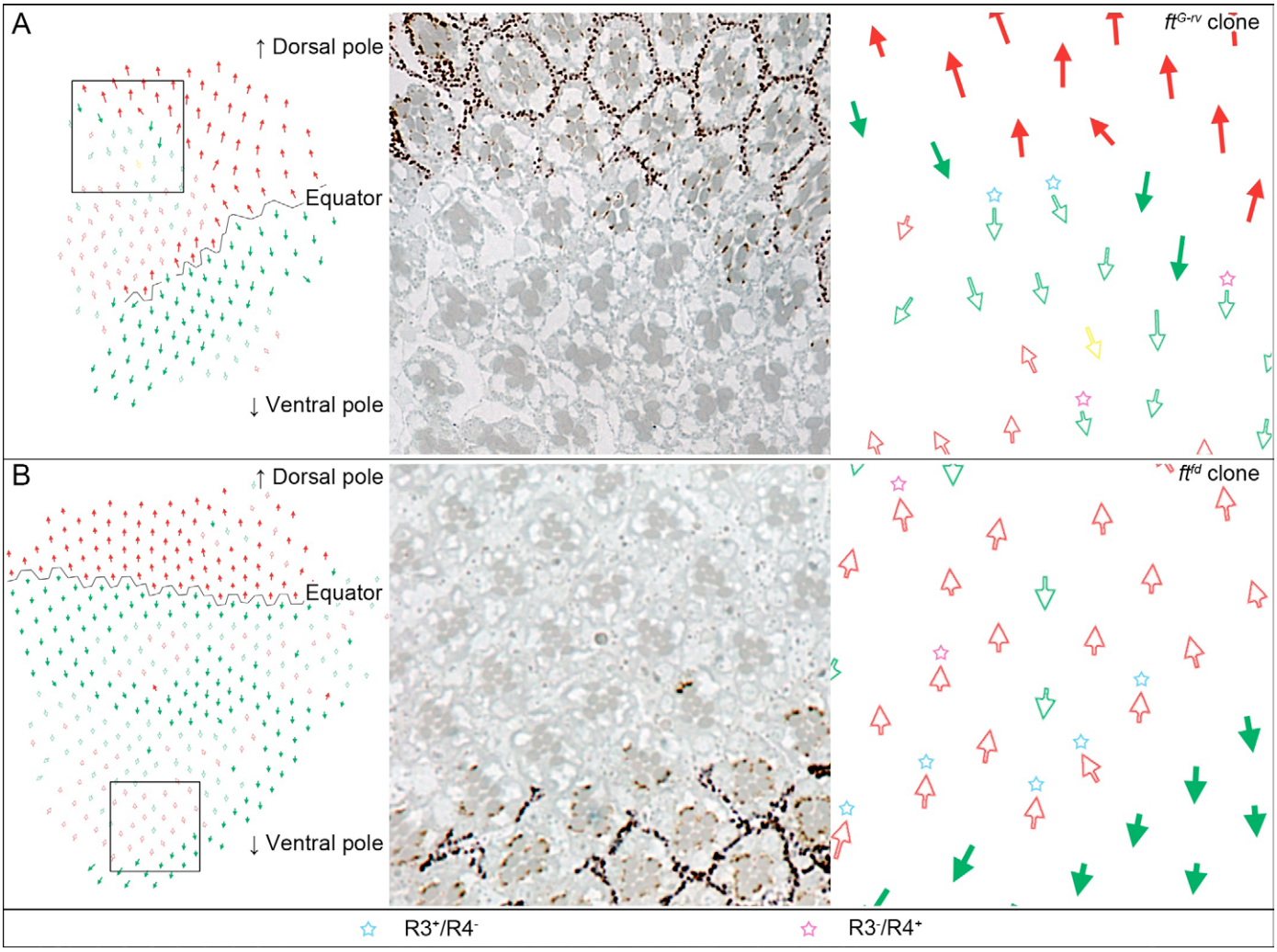

Fig. S2. R3/R4 mosaic ommatidia behave like fully mutant ommatidia in responding to polarity signals. R3/R4 mosaic ommatidia are represented with stars over hollow arrows ($R3^{+}/R4^{-}$: cyan stars, $R3^{-}/R4^{+}$: magenta stars). (**A**) Mosaic ommatidia on the polar border of a $ft^{G\text{-}rv}$ clone have reversed polarity, similarly to their fully mutant neighbors. (**B**) Mosaic ommatidia on the polar border of a ft^{fd} clone have reversed polarity, similarly to their fully mutant neighbors.

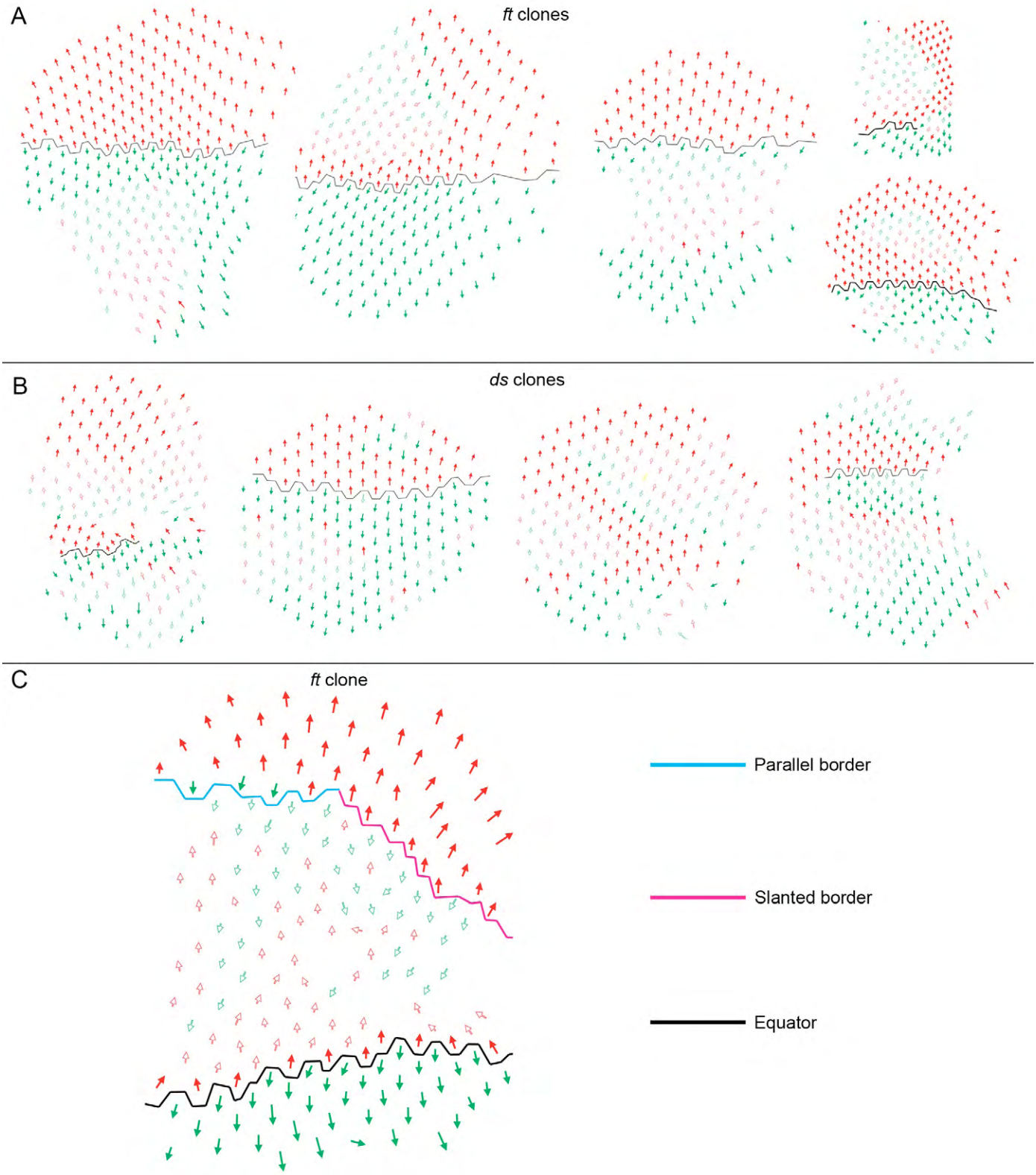

Fig. S3. Polarity information is transmitted inside *ft* and *ds* clones. (**A**) *ft* clones have polarity rescued on the equatorial side, and reversed on the polar side. These effects are strongest near the borders and extend up to several rows. In the middle of the clones these effects are weak or non-existent, and polarity is randomized. (**B**) *ds* clones have polarity rescued on the polar side, and reversed on the equatorial side. The reversal effect of *ds* clones is not as strong as that of *ft* clones, and rarely extends past one ommatidial row. However, the rescue effect is strong, and can extend for multiple rows. (**C**) Example of a *ft* clone indicating clone borders parallel (cyan line) and slanted (magenta line) relative to the equator. This clone shows the general trend of parallel borders to have more reversals than slanted borders.

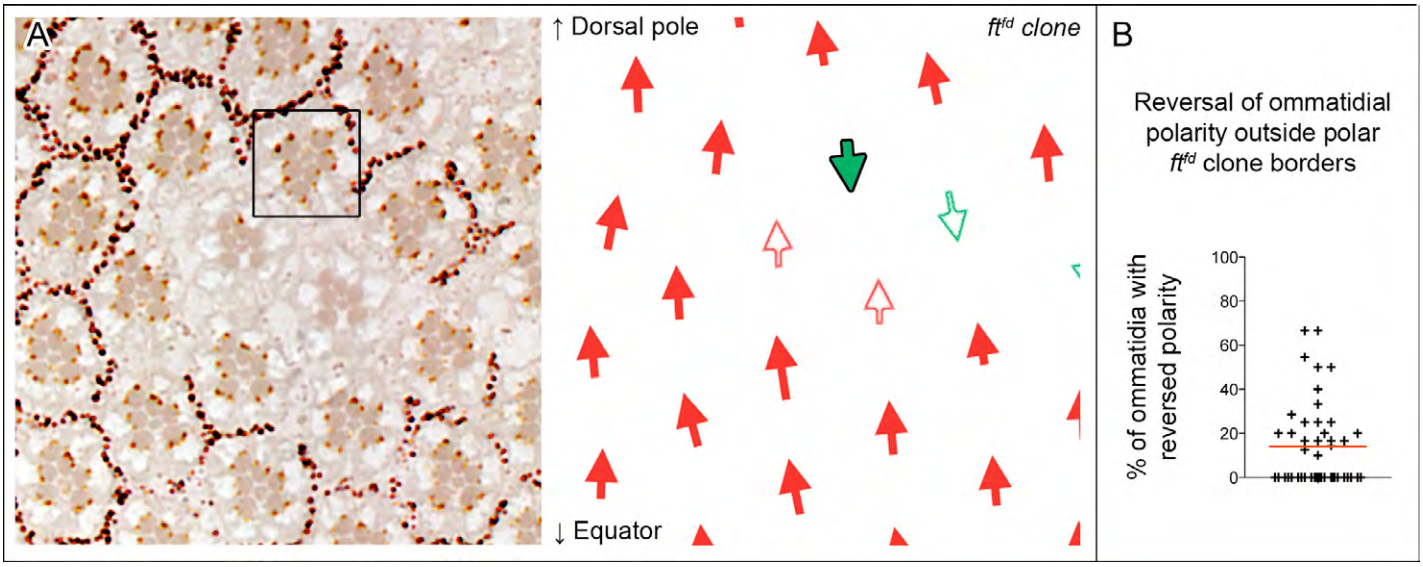

Fig. S4. *ft*^{fd} affects polarity similarly to *ft*$^{G\text{-}rv}$. *ft*^{fd} mutant clones cause polarity reversals in the eye qualitatively similar to *ft*$^{G\text{-}rv}$ mutant clones. (**A**) Polarity reversal of an ommatidium with seven wild-type photoreceptors (in box) on the polar side of a *ft*^{fd} mutant clone. (**B**) Scatterplot of polarity reversals outside polar borders of *ft*^{fd} clones. The mean strength is 14% (*n*=46 clones).

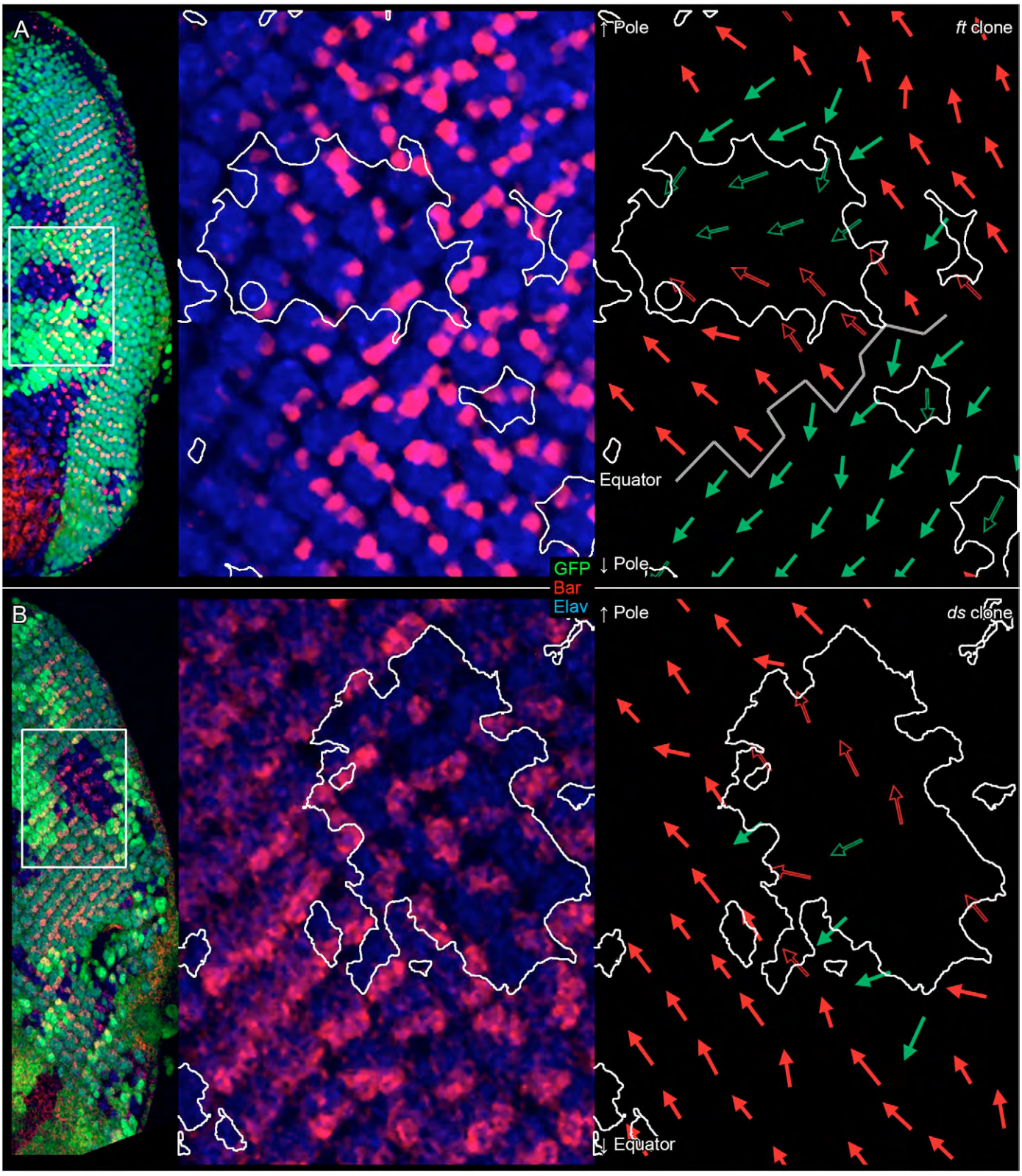

Fig. S5. Polarity disruptions are evident during development in the eye imaginal disc. Elav staining marks all photoreceptors, and Bar staining marks photoreceptors 1 and 6. Loss of GFP marks mutant tissue. Mutant tissue is outlined in white in higher magnifications. (**A**) *ft* clones cause polarity disruptions on the polar side of clones. (**B**) *ds* clones cause polarity disruptions on the equatorial side of clones.

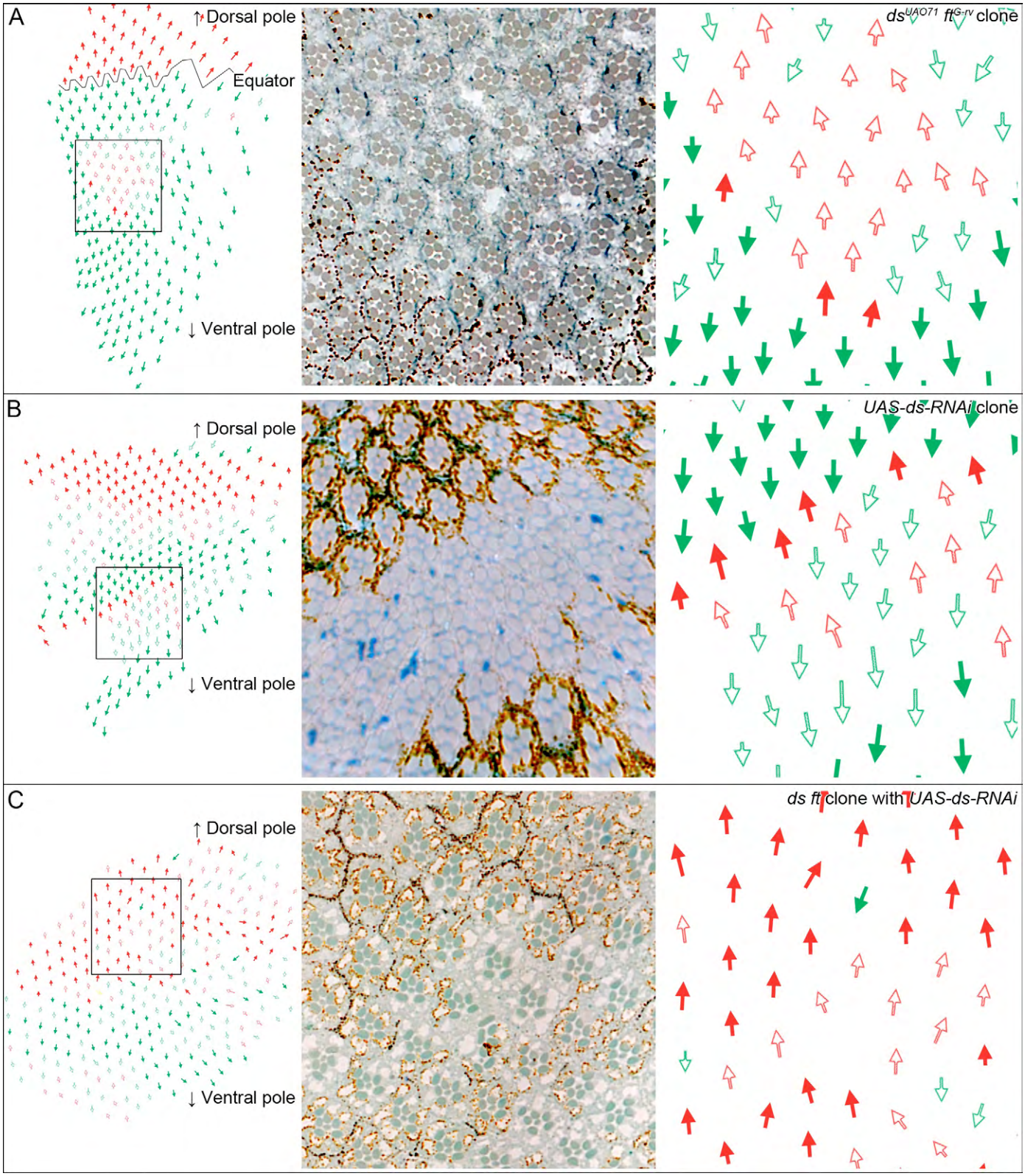

Fig. S6. Residual *ds* function does not cause *ds ft* clonal polarity effects. (**A**) ds^{UAO71} $ft^{G\text{-}rv}$ clones, marked by absence of pigment, show polarity reversals outside clones similarly to ds^{38k} $ft^{G\text{-}rv}$ clones. (**B**) Clones expressing *UAS-ds-RNAi*, marked by absence of pigment, show polarity reversals outside equatorial borders of clones, confirming *ds* knockdown. (**C**) ds^{38k} $ft^{G\text{-}rv}$ clones expressing *UAS-ds-RNAi*, marked by absence of pigment, show polarity reversals outside clones similar to *ds ft* clones not expressing RNAi.

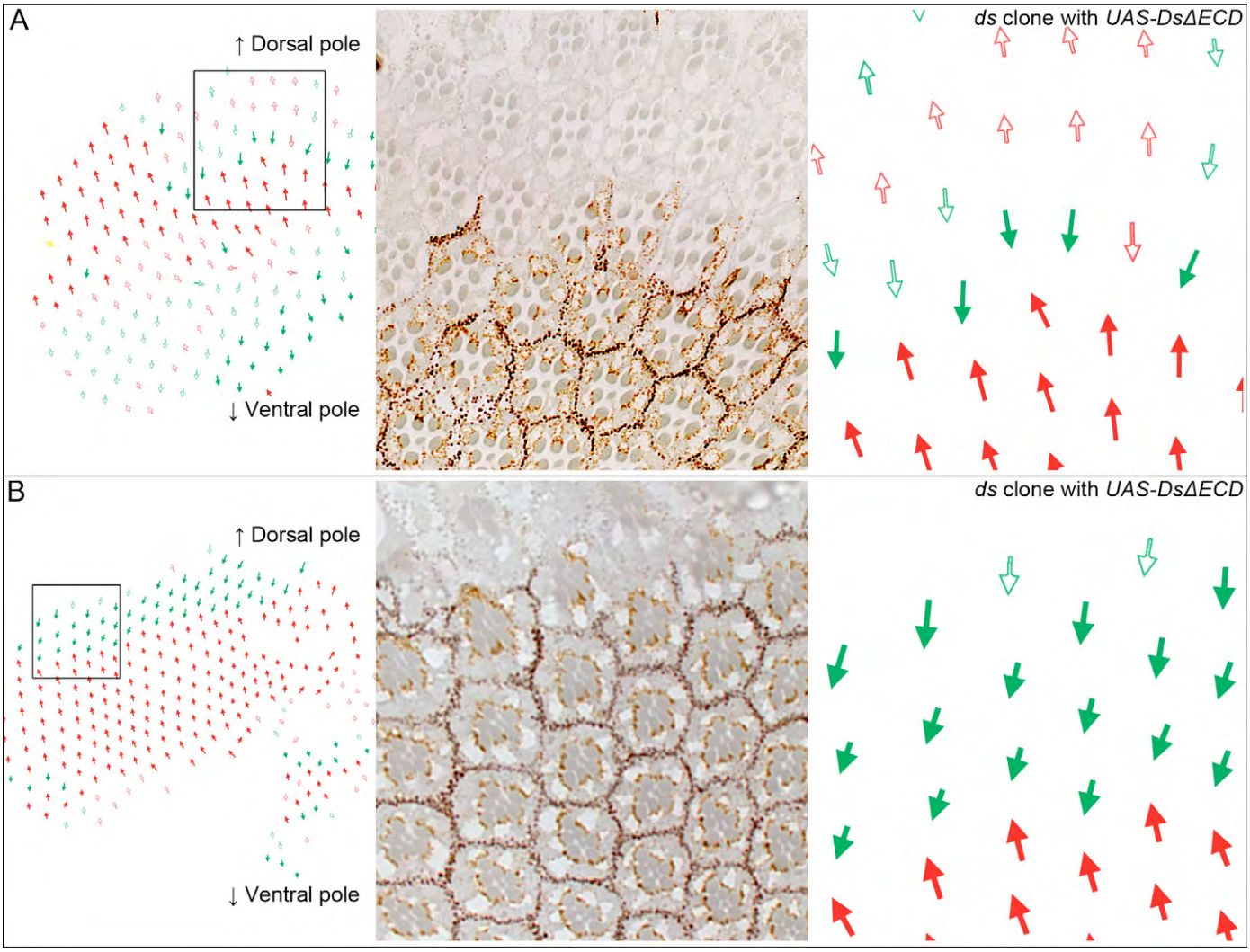

Fig. S7. Expression of DsΔECD strengthens *ds* clonal polarity effects. (**A**,**B**) *ds* mutant clones expressing *UAS-DsΔECD*. There is very strong polarity reversal outside equatorial borders.

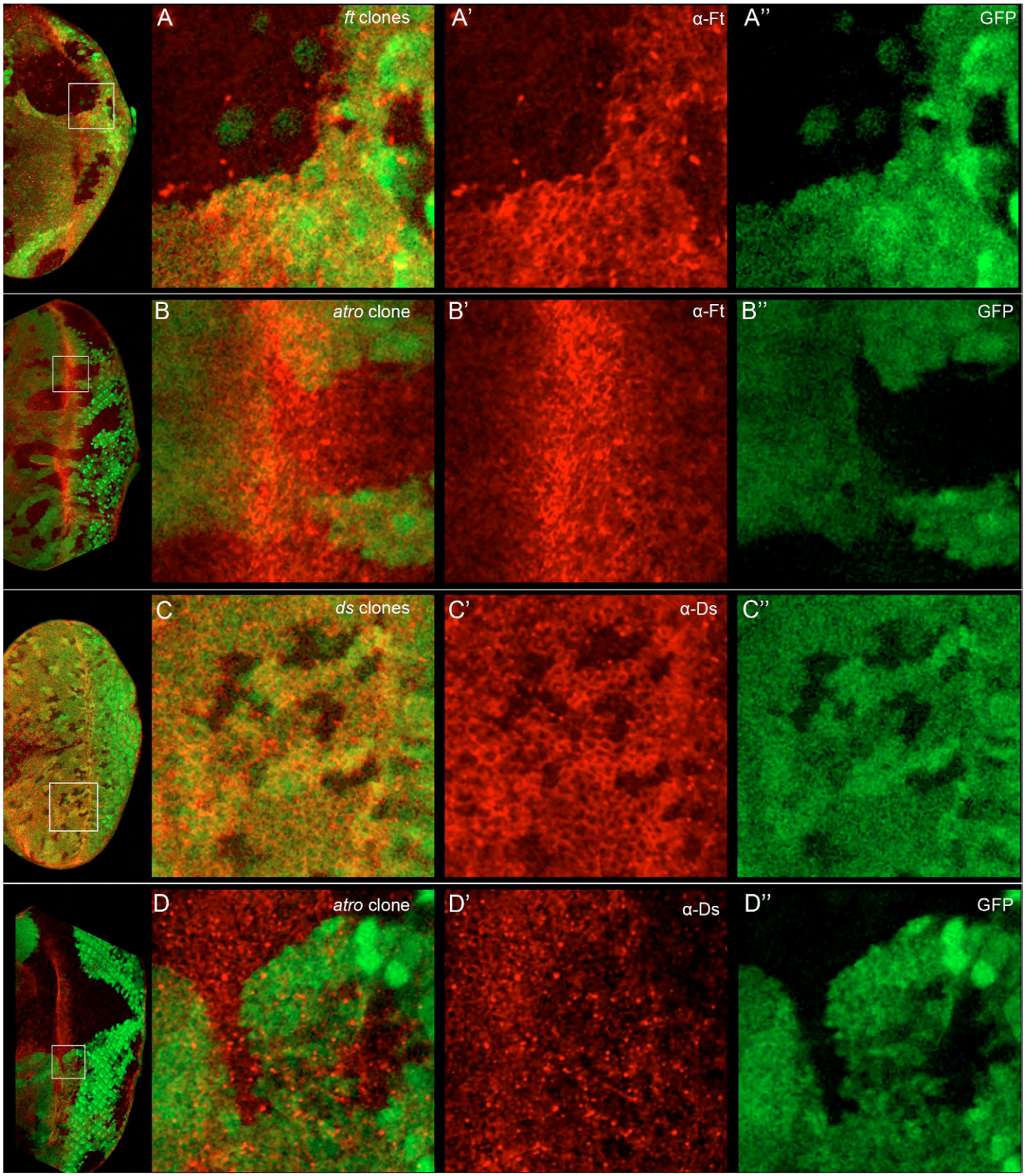

Fig. S8. Ft and Ds levels and localization are not affected by loss of *atro*. (**A-A″**) *ft* mutant clones in eye discs, marked by loss of GFP, show loss of α-Ft staining. (**B-B″**) *atro* mutant clones in eye discs, marked by loss of GFP, do not show changes in α-Ft staining. (**C-C″**) *ds* mutant clones in eye discs, marked by loss of GFP, show loss of α-Ds staining. (B-B″) *atro* mutant clones in eye discs, marked by loss of GFP, do not show changes in α-Ds staining.

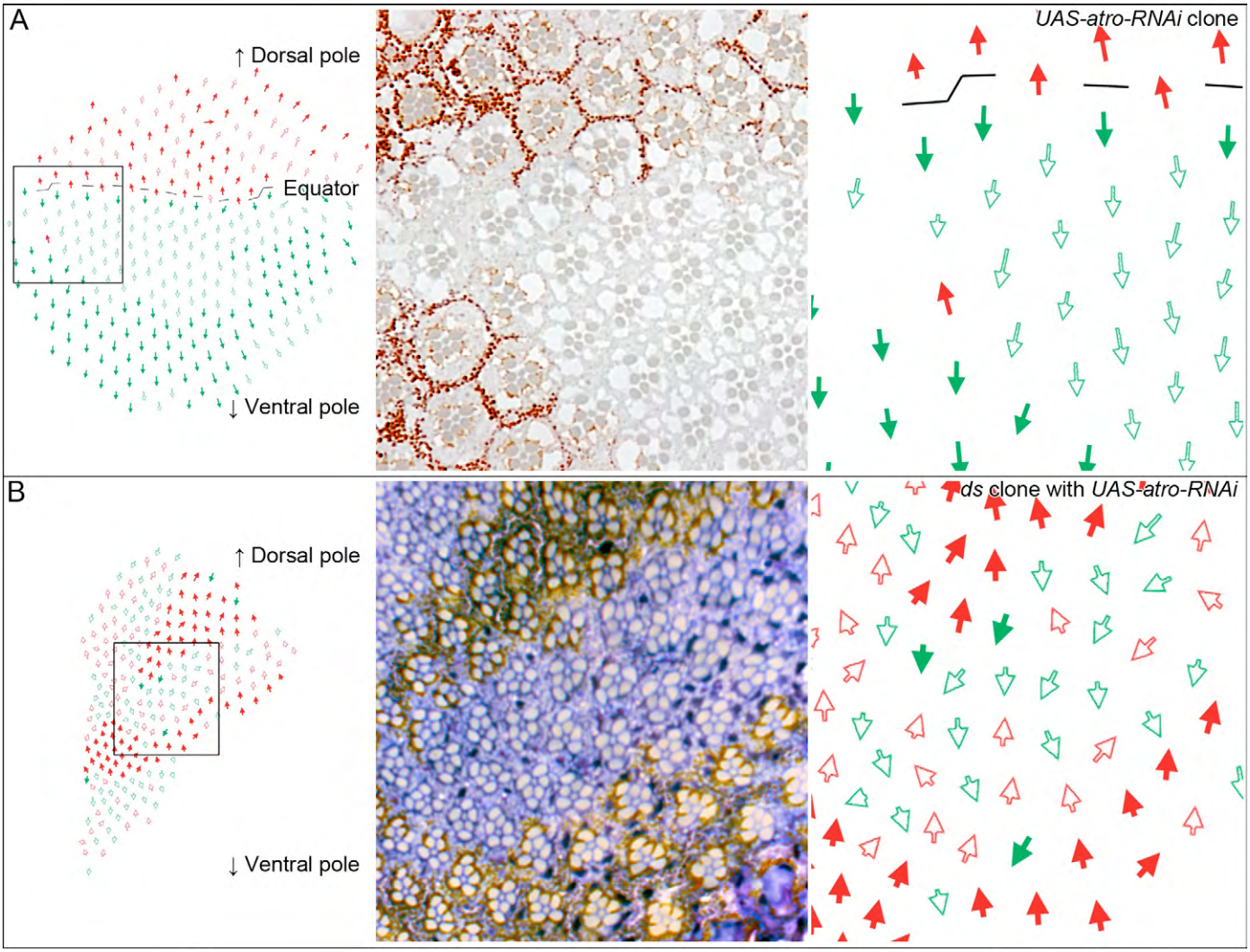

Fig. S9. *ds* clones expressing *UAS-atro-RNAi* cause polar and equatorial polarity reversals. (**A**) Clones expressing *atro-RNAi* occasionally cause polarity reversals in wild-type ommatidia on the polar side. (**B**) Polarity reversals occur in wild-type ommatidia on the polar and, less frequently, equatorial sides of *ds* clones expressing *atro-RNAi*. No clear rescue or reversal of ommatidial polarity is evident inside the clones.

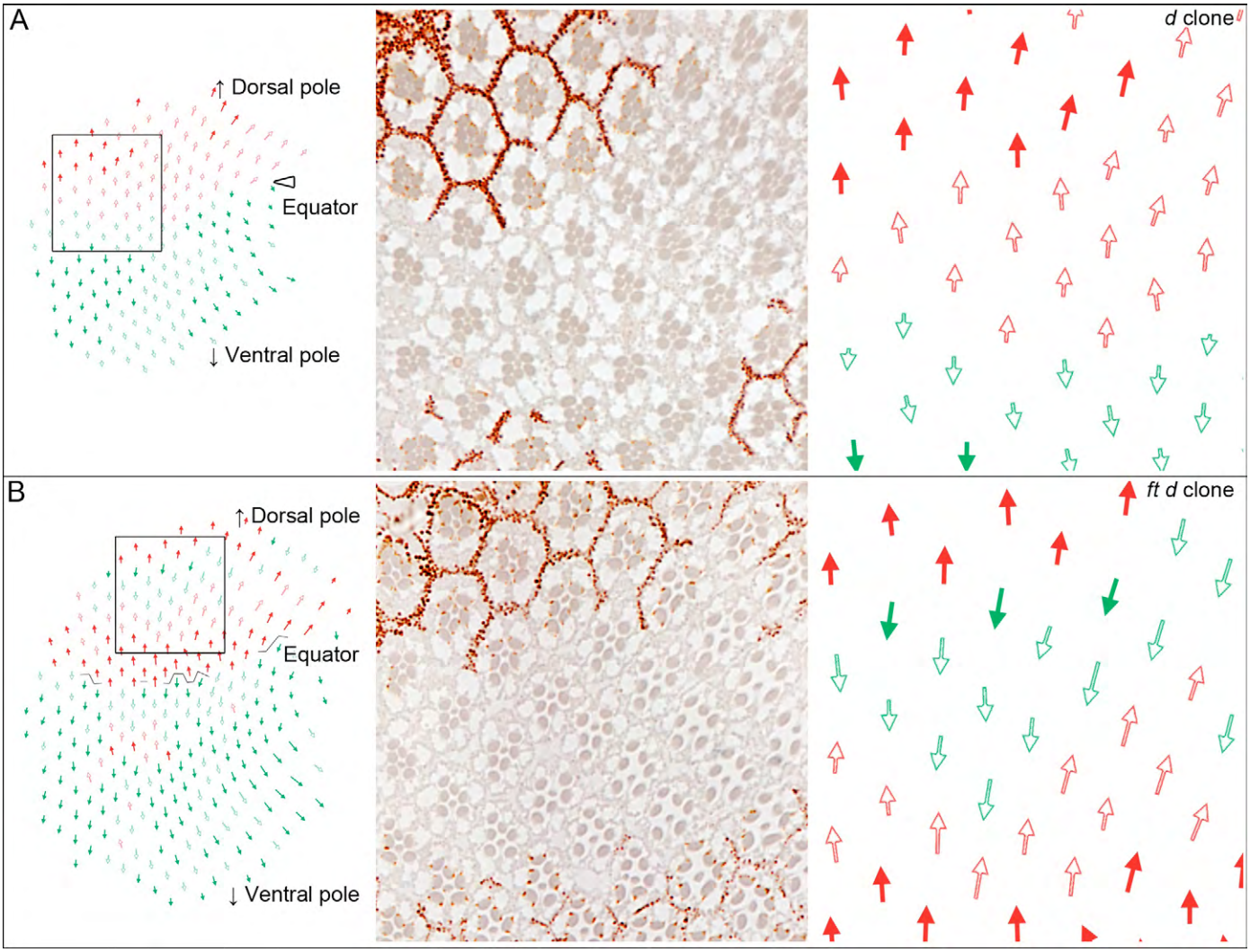

Fig. S10. *d* does not regulate PCP in the eye. (**A**) *d* mutant clones do not disrupt polarity in the eye. As a clone overlaps the equator in this section, the position of the equator is not marked directly on the eye, but is indicated by the arrowhead. (**B**) *ft d* double mutant clones affect polarity inside and outside clones similarly to *ft* mutant clones.

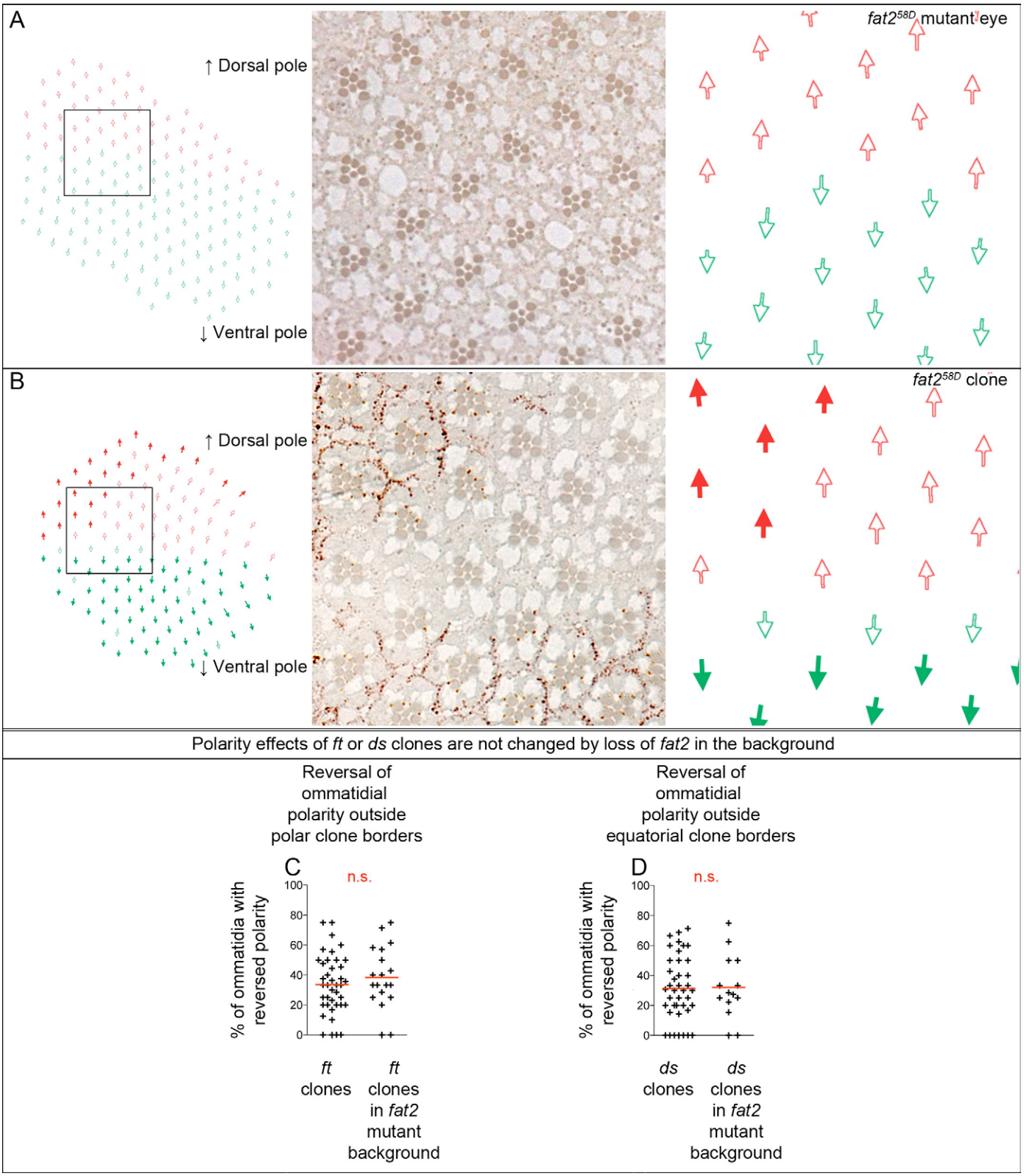

Fig. S11. *fat2* does not regulate PCP in the eye. (**A**) A *fat2* mutant eye. Polarity is normal. (**B**) A *fat2* mutant clone, marked by absence of pigment. No changes in polarity are observed inside or outside the clone. (**C**) *ft* mutant clones in a wild-type background do not differ in strength of polarity reversals outside clones from *ft* mutant clones in a *fat2* mutant background. (**D**) *ds* mutant clones in a wild-type background do not differ in strength of polarity reversals outside clones from *ds* mutant clones in a *fat2* mutant background.

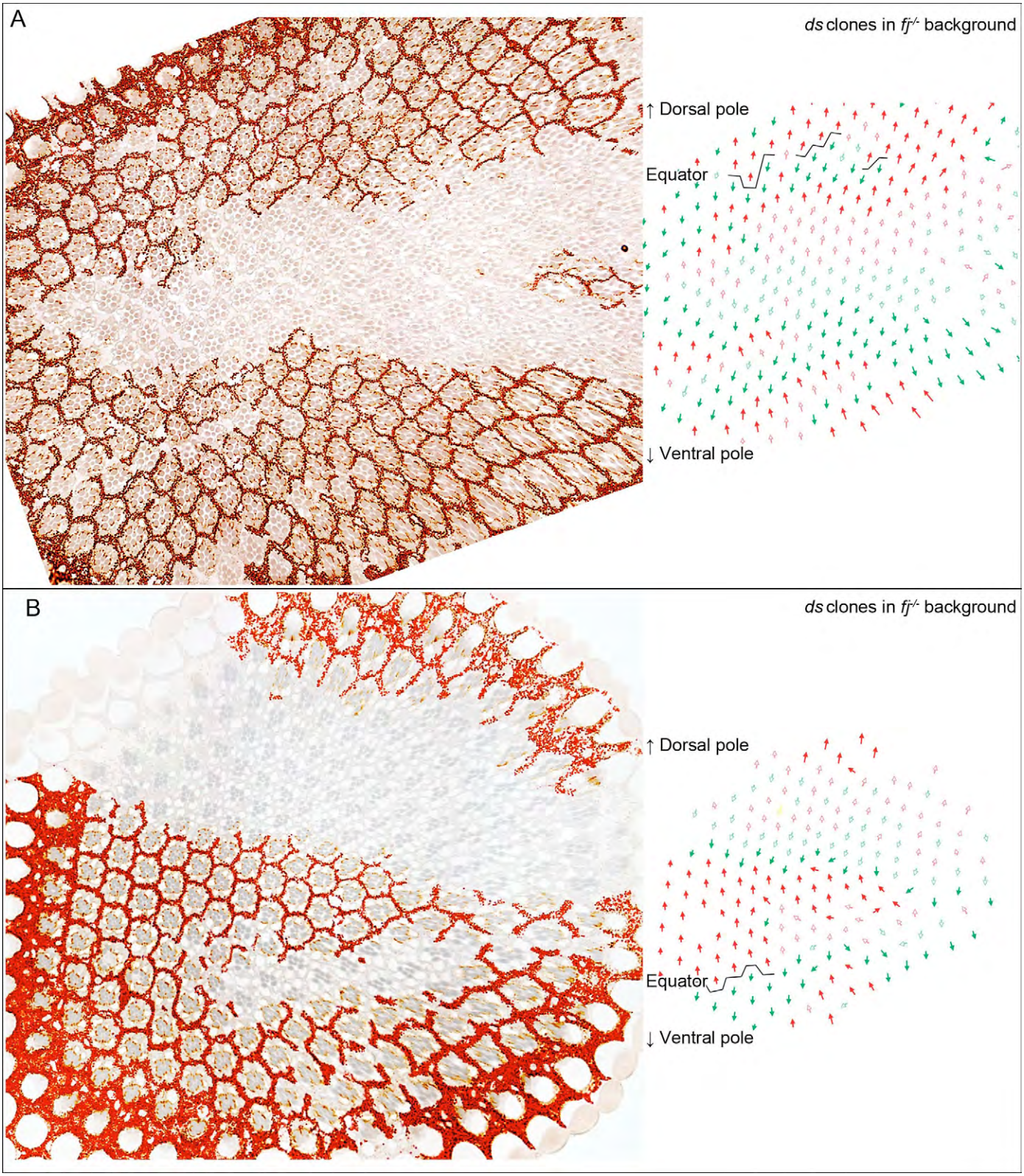

Fig. S12. Loss of *fj* strengthens *ds* clonal polarity reversals. *ds*$^{-}$ clones generated in a *fj*$^{-}$ mutant background show extensive reversal of polarity outside clones, and also reversal and rescue of polarity inside clones, which are missing both *ds* and *fj* gradients.

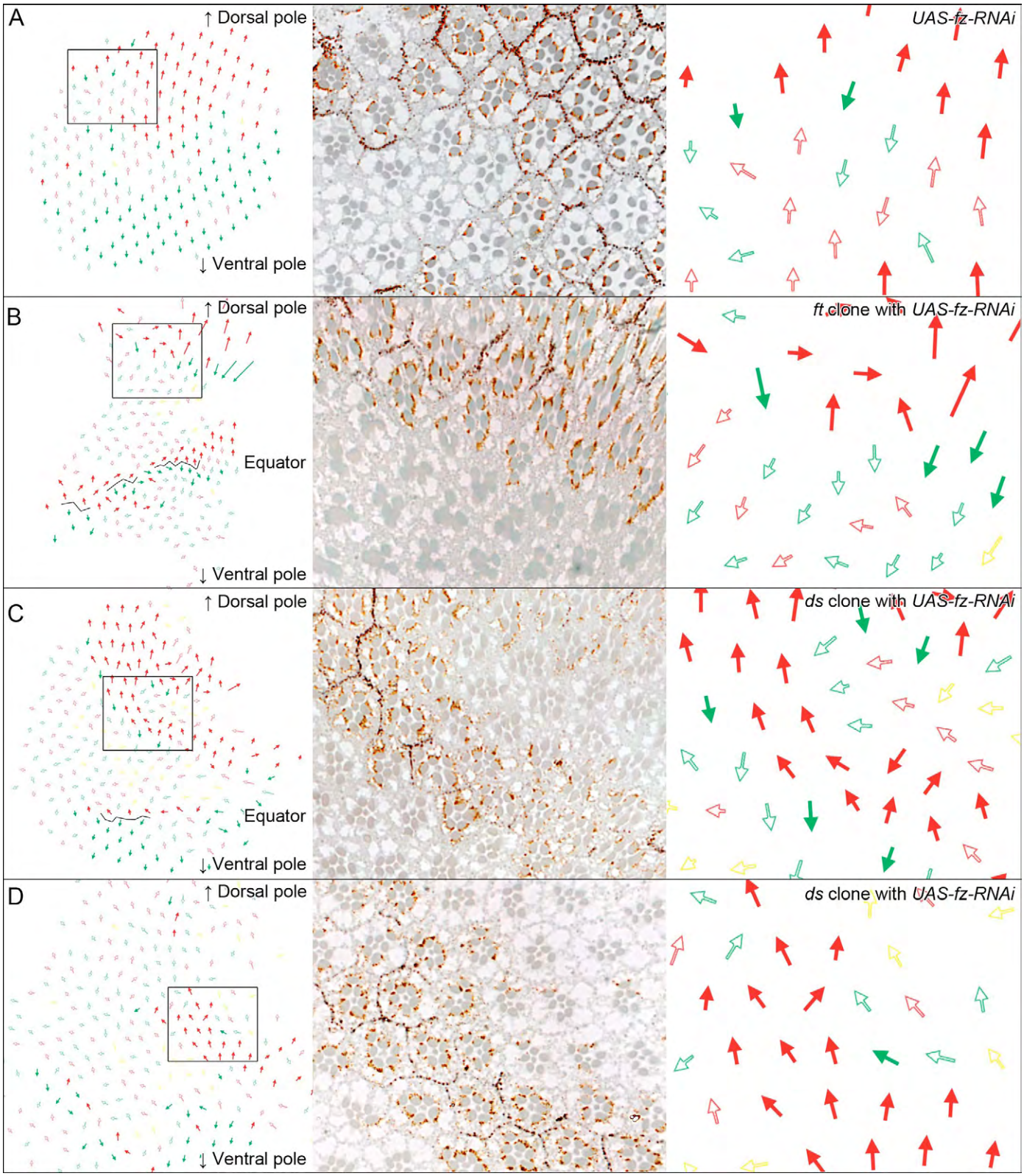

Fig. S13. *ft* or *ds* clones expressing *UAS-fz-RNAi* cause polar polarity reversals. (**A**) Clones expressing *fz-RNAi* cause frequent polarity reversals inside the clone, and occasional reversals in wild-type ommatidia on outside the polar border. (**B**) *ft* clone expressing *fz-RNAi.* There is frequent polarity reversal outside the polar side, and polarity inside clones is disrupted to a greater degree than with *ft* clones, with many more misrotated and symmetrical ommatidia. (**C**,**D**) *ds* clones expressing *fz-RNAi.* There is frequent polarity reversal outside the polar side but only rarely outside the equatorial side of these clones. Furthermore, reversals outside the equatorial side are often associated with misrotation. Polarity inside clones is disrupted to a greater degree than with *ds* clones, with many more misrotated and symmetrical ommatidia.

Table S1. Quantification and comparison of Ft-Ds polarity effects

#	Figure	Clone	Polarity effect	Number of clones	Number of ommatidia	Statistical significance
1	2C, 7A	*ft*$^{-}$	33.58% polar reversal	40	331	
2	2G	*ft*$^{-}$ interior – polar side	88.79% reversal	36	153	Different to random polarity, $P<0.0001$
3	2H	*ft*$^{-}$ interior – equatorial side	92.96% rescue	32	128	Different to random polarity, $P<0.0001$
4	2D	*ft*$^{-}$ – DV size effect	Correlation: $r=0.0028$	36	274	No, $P=0.9872$
5	2E	*ft*$^{-}$ – DV position effect	Correlation: $r=-0.083$	37	282	No, $P=0.6266$
6	2F	*ft*$^{-}$ – parallel border	43.96% polar reversal	36	215	
7	2F	*ft*$^{-}$ – slanted border	13.27% polar reversal	28	107	Different to #6, $P<0.0001$
8	7C	FtΔECD expression	1.563% polar reversal	16	81	
9	7D	*ft*$^{-}$ with FtΔECD expression	26.39% polar reversal	13	71	Not different to #1, $P=0.3086$
10	7B	*ft*$^{-}$ in *fj*$^{-}$ background	62.59% polar reversal	9	65	Different to #1, $P=0.0003$
11	7E	*Fz*-RNAi expression	3.667% polar reversal	10	58	
12	7F	*ft*$^{-}$ with *fz*-RNAi expression	40.24% polar reversal	7	45	Not different to #1, $P=0.4428$
13		*d*$^{-}$	1.818% polar reversal	11	45	
14	7G	*ft*$^{-}$ *d*$^{-}$	31.53% polar reversal	19	127	Not different to #1, $P=0.7153$
15	3B, 7H	*ds*$^{-}$	31.45% equatorial reversal	40	355	
16	3F	*ds*$^{-}$ interior – polar side	95.37% rescue	36	153	Different to random polarity, $P<0.0001$

17	3G	*ds*$^{-}$ interior – equatorial side	65.86% reversal	29	179	Different to random polarity, *P*=0.0046
18	3C	*ds*$^{-}$ – DV size effect	Correlation: *r*=0.34	27	221	No, *P*=0.0872
19	3D	*ds*$^{-}$ – DV position effect	Correlation: *r*=0.46	33	293	Yes, *P*=0.0073
20	3E	*ds*$^{-}$ – parallel border	30.64% equatorial reversal	37	284	
21	3E	*ds*$^{-}$ – slanted border	41.55% equatorial reversal	13	71	Not different to #20, *P*=0.2278
22	7J	DsΔECD expression	4.359% equatorial reversal	26	169	
23	7K	*ds*$^{-}$ with DsΔECD expression	47.60% equatorial reversal	18	120	Different to #15, *P*=0.0230
24	7L	*ft*$^{-}$ with DsΔECD expression – polar border	40.73% polar reversal	7	71	Not different to #1, *P*=0.2757
25	7L	*ft*$^{-}$ with DsΔECD expression – equatorial border	0% equatorial reversal	11	92	N/A
26	7M	*ds*$^{-}$ *ft*$^{-}$ with DsΔECD expression – polar border	6.250% polar reversal	8	42	Not different to #31, *P*=0.3543
27	7M	*ds*$^{-}$ *ft*$^{-}$ with DsΔECD expression – equatorial border	0% equatorial reversal	11	72	N/A
28	7I	*ds*$^{-}$ in *fj*$^{-}$ background	68.07% equatorial reversal	23	112	Different to #15, *P*<0.0001
29	7N	*ds*$^{-}$ with *fz*-RNAi expression – polar border	36.41% polar reversal	14	84	
30	7N	*ds*$^{-}$ with *fz*-RNAi expression – equatorial border	4.177% equatorial reversal	15	114	Different to #15, *P*<0.0001
31	4B, 7O	*ds*$^{-}$ *ft*$^{-}$	2.987% polar reversals	40	288	Different to #1, *P*<0.0001
32	4F	*ds*$^{-}$ *ft*$^{-}$ interior – polar side	38.42% rescue	27	112	Not different to random polarity, *P*=0.0844
33	4G	*ds*$^{-}$ *ft*$^{-}$ interior – equatorial side	72.70% rescue	30	195	Different to random polarity, *P*<0.0001
34	4C	*ds*$^{-}$ *ft*$^{-}$ – DV size effect	Correlation: *r*=0.11	38	277	No, *P*=0.5171

35	4D	*ds*$^{-}$ *ft*$^{-}$ – DV position effect	Correlation: r=0.36	36	267	No, P=0.0335
36	4E	*ds*$^{-}$ *ft*$^{-}$ – parallel border	3.356% polar reversals	36	211	
37	4E	*ds*$^{-}$ *ft*$^{-}$ – slanted border	0.5348% polar reversals	17	77	Not different to #36, P=0.1114
38	7P	*ds*$^{-}$ *ft*$^{-}$ in *fj*$^{-}$ background	15.73% polar reversals	6	43	Different to #31, P=0.0004
39	7Q	*ds*-RNAi expression	47.61% equatorial reversals	4	40	
40	6C, 7R	*Atro*$^{-}$	17.10% polar reversals	38	362	Different to #1, P=0.0003
41	6D	*atro*$^{-}$ – DV size effect	Correlation: r=–0.11	38	362	No, P=0.5265
42	6E	*atro*$^{-}$ – DV position effect	Correlation: r=–0.39	35	314	Yes, P=0.0200
43	6F	*atro*$^{-}$ – parallel border	18.65% polar reversals	34	302	
44	6F	*atro*$^{-}$ – slanted border	8.044% polar reversals	14	66	Not different to #43, P=0.0795
45	7S	*atro*$^{-}$ in *fj*$^{-}$ background	54.65% polar reversals	13	121	Different to #40, P<0.0001
46	7T	*atro*-RNAi	0.4630% polar reversals	9	69	
47	7U	*ds*$^{-}$ with *atro*-RNAi expression– polar border	10.15% polar reversals	29	168	Different to #46, P=0.0333
48	7U	*ds*$^{-}$ with *atro*-RNAi expression – equatorial border	3.627% equatorial reversals	44	302	Different to #15, P<0.0001